Theory of light-induced drift. IV. Models of bulk light-induced drift in three dimensions

Frank O. Goodman*
Department of Applied Mathematics, University of Waterloo, Waterloo, Ontario, Canada N2L 3G1
(Received 6 August 2002; published 30 January 2003)

Light-induced drift (LID) of a rarefied gas in a cell is studied, and exact analytical closed-form solutions to the model rate equations are obtained for bulk LID (BLID) in three dimensions, emphasis being placed on the limit of low radiation absorption by the gas. Comparisons are made with an existing model of BLID in one dimension [F. O. Goodman, preceding paper, Phys. Rev. A **67**, 013410 (2003)], and we examine whether there are any conditions under which that model is satisfactory. Comparisons are also made with the author's models of surface LID in one dimension (above reference) and in three dimensions [F. O. Goodman, Phys. Rev. A **65**, 063409 (2002); **65**, 063410 (2002)].

DOI: 10.1103/PhysRevA.67.013411 PACS number(s): 34.50.Rk

I. INTRODUCTION

In part III of this series of papers [1–3], the phenomenon of light-induced drift (LID) was discussed, and exact treatments of models of surface and bulk LID (SLID and BLID, respectively), in one dimension (1D) were presented and compared. Here (''here'' means ''in the present paper'') we consider a model of BLID in three dimensions (3D), and are able to examine whether there are any conditions under which the simpler 1D model of BLID is satisfactory. In parts I and II, models of SLID in 3D were presented, and we are able here to compare results for BLID and SLID in 3D; for completeness, we also compare with results from part III for SLID in 1D.

As before [2,3], in order to understand the material here it is necessary for readers to have read and understood part I, and of course an understanding of parts II and III is also necessary. References to entities in earlier parts are made here with the notation (I.5.7), (III.3.5), and so on. Unless otherwise stated, symbols used here have the same meanings as those in part III.

Dimensionless (unasterisked) variables are formed from dimensional (asterisked) variables as in part III, that is, we have

$$\hbar\omega = \chi = b = 2T/\mu = 1, \tag{1.1}$$

where $\hbar^*$ is Planck's constant, ω^* is the laser frequency, χ^* is a characteristic length associated with the cell, b^* is the Boltzmann constant, T^* is the temperature, and μ^* is the gas molecular mass. As in part III, the choice of χ^* for the characteristic length implies that the dimensionless average inverse mean free path for molecule–buffer-particle collisions is given by $\theta = \theta^*\chi^*$, and θ is carried through the analysis. As in earlier parts, essentially all useful information is contained in the three integrals I_{1e}, I_{xs}, and I_{qd}, particularly in the ratios [4] I_{qd}/q_0, I_{xs}/I_{qd}, and I_{1e}/I_{qd}.

In order to write results in concise form, we need to make additional definitions of quantities analogous to the definitions of $d(\exp)$, $D(\mathrm{erf})$, dG_ξ, and so on, already made in parts I–III, and these are collected together in Appendix A, together with some explanation of the origins of some of the names used therein; the reasons for making these perhaps peculiar-looking definitions will become clear when exact results are presented below. For clarity here, some of the earlier definitions are repeated in Appendix A.

II. ANALYSIS OF 3D BLID

We start the analysis in n dimensions (nD) because we wish to point out the interesting fact that the only values of n for which a reasonably tractable exact analytical model of BLID may be made are $n=1$ and 3, with the case $n=1$ having been studied already in part III. Because of the special nature of the single component v_x of gas molecule velocity (parallel to the laser beam), and the essential appearance of the speed v, it is convenient in nD BLID calculations ($n>1$) to work with the two variables (v_x, v) where $\mathbf{v}=(v_x, v_y, \ldots, v_n)$ and $v=|\mathbf{v}|$. The bulk Maxwellian distribution $m^{(n)}(\mathbf{v})$, in n variables v_k, is given by

$$m^{(n)}(\mathbf{v}) = \pi^{-n/2} e^{-v^2}, \quad -\infty < v_k < \infty, \tag{2.1}$$

from which it follows that our modified distribution, in two variables, is given, for $n>1$, by

$$m^{(n)}(v_x, v) = \frac{2(v^2 - v_x^2)^{(n-3)/2} v e^{-v^2}}{\pi^{1/2}\Gamma((n-1)/2)},$$

$$0 \leqslant v < \infty, \quad -v \leqslant v_x \leqslant v. \tag{2.2}$$

It is the appearance of the exponent $(n-3)/2$ in Eq. (2.2) that is the origin of our remarks above concerning the tractability (unique for $n>1$) of the case $n=3$, for which

$$m(v) \equiv m^{(3)}(v_x, v) = 2\pi^{-1/2} v e^{-v^2}, \tag{2.3}$$

where we note that v_x does not appear explicitly in $m \equiv m^{(3)}$.

We now specialize to the case $n=3$. The working follows that of Sec. III A of part III down to (III.3.5), with, for the

*Also at Department of Physics, University of Waterloo, and the Guelph-Waterloo Physics Institute, Ontario, Canada.

TABLE I. The limits for the 24 subintegrals, that is, the six subintegrals for each of the four cases A–D discussed in Sec. II. The subscripts *i,o* on the v_x limits indicate, in an obvious notation, which of $F_j^{(\mathrm{in})}, F_j^{(\mathrm{out})}$ is involved. In the v limits, min $\equiv \min(|v_a|,|v_b|)$ and max $\equiv \max(|v_a|,|v_b|)$. Examples of the use of the table are given in Eqs. (2.6) and (2.7).

$v^{(\mathrm{A-D})}$	$v_x^{(\mathrm{A})}$	$v_x^{(\mathrm{B})}$	$v_x^{(\mathrm{C})}$	$v_x^{(\mathrm{D})}$
(0, min)	$(-v,v)_o$	$(-v,v)_i$	$(-v,v)_i$	$(-v,v)_o$
(min, max)	$(-v,v_a)_o$		$(-v,v_b)_i$	
	$(v_a,v)_i$		$(v_b,v)_o$	
(max, ∞)		$(-v,v_a)_o$		
		$(v_a,v_b)_i$		
		$(v_b,v)_o$		

distributions $f_j(v_x,v)$ for the ground state ($j\equiv g$) and excited state ($j\equiv e$), the 3D (steady-state) substitution

$$f_j(v_x,v)=F_j(v_x,v)m(v) \tag{2.4}$$

used instead of the 1D version which comes from (III.2.1) and (III.2.2). The analogs of the results (III.3.10) are found by calculating the integrals (2.5) below, in which the excitation-frequency function $q(v_x)$ is again written $q(v_x)=q_0\Delta h$ with q_0 constant and the interval Δh defined by (III.2.6). We use the style $F_j(v_x,v)$ for F_j to remind us that it depends both on v and on whether or not v_x lies in the excitation interval $[v_a,v_b]$. The required integrals are as follows:

$$I_{1j}=\int_0^\infty dv\, m(v)\int_{-v}^{v} dv_x F_j(v_x,v), \tag{2.5a}$$

$$I_{qj}=q_0\int_0^\infty dv\, m(v)\int_{-v}^{v} dv_x \Delta h F_j(v_x,v), \tag{2.5b}$$

$$I_{vj}=\int_0^\infty dv\, m(v) v\int_{-v}^{v} dv_x F_j(v_x,v), \tag{2.5c}$$

$$I_{xj}=\int_0^\infty dv\, m(v)\int_{-v}^{v} dv_x v_x F_j(v_x,v). \tag{2.5d}$$

Because of the difference between $F_j^{(\mathrm{in})}$ and $F_j^{(\mathrm{out})}$, it is convenient to rewrite each of the integrals (2.5) as a sum of six subintegrals, the limits for which depend on v_a,v_b. There are four different cases (A–D) to consider, bearing in mind that $v_a<v_b$: (A) $0\leqslant v_a<v_b$, (B) $v_a\leqslant 0<v_b$ with $|v_a|<v_b$, (C) $v_a<0\leqslant v_b$ with $|v_a|>v_b$, and (D) $v_a<v_b\leqslant 0$. The limits for the 24 subintegrals (six for each case) are given in Table I, and the first steps in two examples will help readers interpret Table I, as follows.

The first subintegral for case A has v limits $(0,\min)=(0,|v_a|)=(0,v_a)$ and v_x limits $(-v,v)_o$, thus involving $F_j^{(\mathrm{out})}$, so that, for example, the first subintegral $I_{vj}^{(1)}$ contribution to I_{vj} in this case is

$$I_{vj}^{(1)}=\int_0^{v_a} dv\, m(v) v\int_{-v}^{v} dv_x F_j^{(\mathrm{out})} \tag{2.6a}$$

$$=4\pi^{-1/2}\int_0^{v_a} dv\, v^2 e^{-v^2}[S_j+2Z_j/(v+g)]. \tag{2.6b}$$

The second subintegral for case C has v limits $(\min,\max)=(|v_b|,|v_a|)=(v_b,-v_a)$ and v_x limits $(-v,v_b)_i$, thus involving $F_j^{(\mathrm{in})}$, so that, for example, the second subintegral $I_{xj}^{(2)}$ contribution to I_{xj} in this case is

$$I_{xj}^{(2)}=\int_{v_b}^{-v_a} dv\, m(v)\int_{-v}^{v_b} dv_x v_x F_j^{(\mathrm{in})} \tag{2.7a}$$

$$=\pi^{-1/2}\int_{v_b}^{-v_a} dv\, v(v_b^2-v^2)e^{-v^2}[S_j+2W_j/(v+w)]. \tag{2.7b}$$

In order to help readers in working through the four cases, the complete results for case A are given in Appendix B.

The exact solution in each case is now obtained by solving the system of (five) equations

$$c_j=I_{1j},\quad c_j\beta_j=\tfrac{1}{2}\pi^{1/2}I_{vj},\quad c_g+c_e=1 \tag{2.8}$$

for the (four) quantities c_j,β_j. The general exact results for the important quantities are readily obtained from the procedure described above, but are too long to be usefully presented here [5]. However, with use of the definitions in Appendix A, useful exact results for the double limits $(\gamma,q_0)\to(0,0)$, where γ is the spontaneous decay rate parameter, which apply not only to all four cases (A–D), but to general values of v_a,v_b with $v_a\neq v_b$, may be made surprisingly simple, and are presented in Table II, together with the analogous exact results for 1D BLID and SLID [3] and 3D SLIDCC [2] where the CC indicates circular-cylindrical cell geometry. The analogous double limit does not exist for 3D SLID with flat-plate cell geometry [1], or for I_{1e} in 1D BLID [3]. If $v_a>v_b$, then the laser excitation interval of v_x is, of course, $[v_b,v_a]$ instead of $[v_a,v_b]$.

A popular [1–3,6] special case is that $(v_a,v_b)=(0,\infty)$, and exact results for this case, again with the double limit $(\gamma,q_0)\to(0,0)$, are shown in Table III.

In order to use Table II to get results for the case $dv\to 0$, with $(v_a,v_b)=(v_L-dv/2,v_L+dv/2)$, that is, analogs of, for example, (III.2.19b), (III.3.16b), and (III.3.17b), we make additional interpretations, analogous to those made in (I.5.7) and (III.3.14), all of which follow from the definitions in Appendix A.

As we see below, it is useful to define a function $\phi(v)$ by

$$\phi(v)=\pi^{1/2}v(1-\mathrm{erf}|v|)e^{v^2} \tag{2.9}$$

which is shown in Fig. 1. The expansions of $\phi(v)$ for small and large $|v|$ may be written as follows:

$$\mathrm{sgn}(v)\,\phi(v)=\pi^{1/2}|v|-2v^2+\pi^{1/2}|v|^3+O(v^4), \tag{2.10a}$$

TABLE II. Exact results for 3D BLID (here), 1D BLID and SLID [3], and 3D SLIDCC [2] for general values of v_a, v_b with $v_a \neq v_b$. For I_{qd}/q_0, the limits with $q_0 \to 0$ are shown; for the other two quantities, the double limits with $(\gamma, q_0) \to (0,0)$ are shown. The indicated double limit does not exist in 3D SLIDFP [1] or for I_{1e} in 1D BLID [3], which is the reason for the blank entry. The limit $q_0 \to 0$ is not in fact needed in the second and third entries for 1D SLID.

Quantity	3D BLID	1D BLID	1D SLID	3D SLIDCC
$\frac{I_{qd}}{q_0}$	$\frac{\lvert d(\mathrm{erf})\rvert}{2}$	$\frac{\lvert d(\mathrm{erf})\rvert}{2}$	$\frac{\lvert d(\mathrm{erf})\rvert}{2}$	$\frac{\lvert d(\mathrm{erf})\rvert}{2}$
$\frac{\alpha_g \alpha_e}{\Delta\alpha}\frac{I_{xs}}{I_{qd}}$	$\frac{\pi^{-1/2} D(v\ \exp) + d(v^2\ \mathrm{erf\ C}) + (1/2) D(\mathrm{erf})}{\theta d(\mathrm{erf})}$	$\frac{D(\mathrm{erf})}{\theta d(\mathrm{erf})}$	$\frac{d(\exp)}{d(\mathrm{erf})}$	$\frac{\pi}{2}\frac{d(\exp)}{d(\mathrm{erf})}$
$\alpha_e \frac{I_{1e}}{I_{qd}}$	$\frac{\psi}{2\theta} + \frac{2\pi^{-1/2} d(\exp\ \mathrm{C\ sgn}) + 2d(v\ \mathrm{erf\ C})}{\theta d(\mathrm{erf})}$		$\psi + \pi^{-1/2}$	$\psi + \frac{\pi^{3/2}}{2}$

$$\mathrm{sgn}(v)\,\phi(v) = 1 - 1/2v^2 + 3/4v^4 + O(1/v^6). \quad (2.10b)$$

Exact results for the triple limit $(\gamma, q_0, dv) \to (0,0,0)$ are given in Table IV.

III. DISCUSSION AND CONCLUSION

For SLID, the 1D model gives a reasonable approximation to the 3D model with CC geometry, the differences involving just two factors of $\pi/2$ (Table II). The same is not true for BLID, in which the 1D model gives unacceptable results (except for I_{qd}/q_0, for which all the models agree). We have already established that the 1D BLID model is unacceptable for calculations of I_{1e}/I_{qd}, and the situation is similar for calculations of I_{xs}/I_{qd}, as is made clear from comparison of Figs. 2 and 3. Figure 2 shows exact results in 1D BLID as a function of v_b for three values of v_a, and Fig. 3, which contains analogous results in 3D BLID, shows clearly how the curves separate smoothly in the realistic 3D case.

Figure 4 shows analogous results in 3D BLID for the other important ratio I_{1e}/I_{qd} for $z=1$ $(\psi=0)$, where z is the fraction of excited-state molecules that are quenched to the ground state during diffuse scattering. The corner that is evident in the curve for $v_a=0$ looks suspicious at first, but is consistent with the following result, which is exact for sufficiently small $|dv|$ in the double limit $(\gamma, q_0) \to (0,0)$ with $v_a = 0$:

TABLE III. Analog of Table II for $(v_a, v_b) = (0, \infty)$.

Quantity	3D BLID	1D BLID	1D SLID	3D SLIDCC
$\frac{I_{qd}}{q_0}$	1/2	1/2	1/2	1/2
$\frac{\alpha_g \alpha_e}{\Delta\alpha}\frac{I_{xs}}{I_{qd}}$	$\frac{1}{2\theta}$	$\frac{1}{\theta}$	1	$\frac{\pi}{2}$
$\alpha_e \frac{I_{1e}}{I_{qd}}$	$\frac{(1/2)\psi + 2\pi^{-1/2}}{\theta}$		$\psi + \pi^{1/2}$	$\psi + \frac{\pi^{3/2}}{2}$

$$\theta \alpha_e I_{1e}/I_{qd} = \tfrac{1}{2}\psi + \pi^{1/2} - |dv| + O((dv)^2). \quad (3.1)$$

As with the models presented [1–3] in parts I–III, numerical results may be obtained by iteration of the analytical steady-state equations, and, independently, by integration of the Maxwell-Boltzmann rate equations with respect to time. Implementation of these procedures is described most thoroughly in part I, and is not discussed further here.

We conclude that, as attractive as it seems at first sight, the 1D model [3] is not generally useful for calculations of BLID, although it may be qualitatively correct in special cases, as in some results (Table III) for $(v_a, v_b) = (0, \infty)$, for example. Physically, this situation is related to the fact that, as we have already discussed in Sec. II, the 1D model (as opposed to an nD model with $n>1$) is very special: the single velocity component v_x both (i) is completely responsible for the molecule–buffer-particle collisions (of frequency $\theta|v_x|$) and (ii) contains the laser excitation interval $(v_a \leqslant v_x \leqslant v_b)$; with $n>1$, it is v, rather than just v_x, that is responsible for the collisions (of frequency θv) giving qualitatively different results generally.

The same is not true of the 1D model of SLID [3], in which motion orthogonal to v_x must be superimposed artifi-

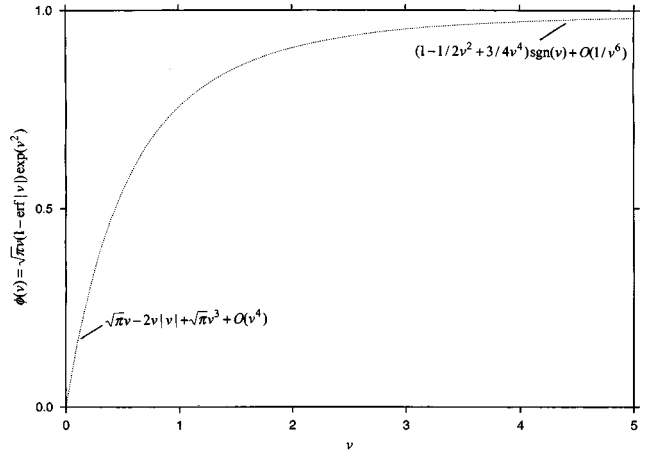

FIG. 1. The function $\phi(v)$ defined by Eq. (2.9). We note that $\phi(v)$ is an odd function of v with the expansions (2.10) as shown.

TABLE IV. Analog of Table II for $(v_a, v_b) = (v - dv/2, v + dv/2)$ with the additional limit $dv \to 0$. We note that v in this table stands for v_L in the text. The limit $q_0 \to 0$ is not in fact needed in the second entry for 1D BLID in this case.

Quantity	3D BLID	1D BLID	1D SLID	3D SLIDCC
$\frac{I_{qd}}{q_0 dv}$	$\frac{e^{-v^2}}{\pi^{1/2}}$	$\frac{e^{-v^2}}{\pi^{1/2}}$	$\frac{e^{-v^2}}{\pi^{1/2}}$	$\frac{e^{-v^2}}{\pi^{1/2}}$
$\frac{\alpha_g \alpha_e}{\Delta\alpha} \frac{I_{xs}}{I_{qd}}$	$\frac{\phi(v)}{\theta}$	$\frac{\mathrm{sgn}(v)}{\theta}$	$\pi^{1/2} v$	$\frac{\pi^{3/2} v}{2}$
$\alpha_e \frac{I_{1e}}{I_{qd}}$	$\frac{(1/2)\psi + \phi(v)/v}{\theta}$		$\psi + \pi^{1/2}$	$\psi + \frac{\pi^{3/2}}{2}$

cially (in order to get molecule-surface collisions). In this sense, a true 1D model of SLID cannot be made, but the fake one [3] does give results that are quite similar to those of the 3D model [2] (for CC geometry).

ACKNOWLEDGMENT

The work was supported by the Natural Sciences and Engineering Research Council of Canada.

APPENDIX A: DEFINITIONS USED HERE

In the following definitions, ξ stand for a, g, or w:

$$\psi = \pi^{1/2}(1-z)/z, \tag{A1}$$

$$v_L = (v_b + v_a)/2, \tag{A2}$$

$$dv = v_b - v_a, \tag{A3}$$

$$G_\xi = G(\xi), \tag{A4}$$

$$G_{c\xi} = G(v_c, \xi), \quad c \equiv a \text{ or } b, \tag{A5}$$

$$dG_\xi = G_{b\xi} - G_{a\xi}, \tag{A6}$$

$$d(v^2) = v_b^2 - v_a^2, \tag{A7}$$

$$d(\mathrm{erf}) = \mathrm{erf}\, v_b - \mathrm{erf}\, v_a, \tag{A8}$$

$$d(\exp) = e^{-v_a^2} - e^{-v_b^2}, \tag{A9}$$

$$D(\mathrm{erf}) = \mathrm{erf}|v_b| - \mathrm{erf}|v_a|, \tag{A10}$$

$$D(v\ \exp) = |v_a| e^{-v_a^2} - |v_b| e^{-v_b^2}, \tag{A11}$$

$$d(v\ \mathrm{erf}\, C) = v_b(1 - \mathrm{erf}|v_b|) - v_a(1 - \mathrm{erf}|v_a|), \tag{A12}$$

$$d(v^2\ \mathrm{erf}\, C) = v_b^2(1 - \mathrm{erf}|v_b|) - v_a^2(1 - \mathrm{erf}|v_a|), \tag{A13}$$

$$d(\exp C\ \mathrm{sgn}) = (1 - e^{-v_b^2})\mathrm{sgn}(v_b) - (1 - e^{-v_a^2})\mathrm{sgn}(v_a), \tag{A14}$$

where the order of the a, b terms in Eqs. (A9) and (A11) must be noted; this unusual (and, with hindsight, unfortunate) ordering originated in part I in order to make $d(\exp) > 0$ when $0 \leqslant v_a < v_b$ (case (A) here).

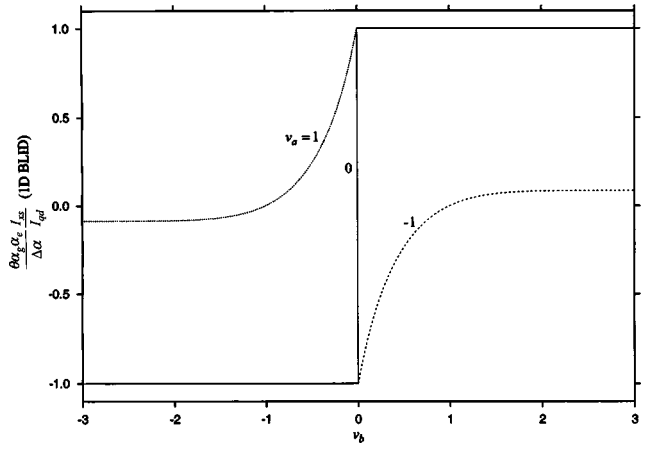

FIG. 2. Exact results (Table II) for I_{xs}/I_{qd} in 1D BLID as a function of v_b with $v_a = -1$, 0, 1, in the double limit $(\gamma, q_0) \to (0,0)$. All other parameters are arbitrary.

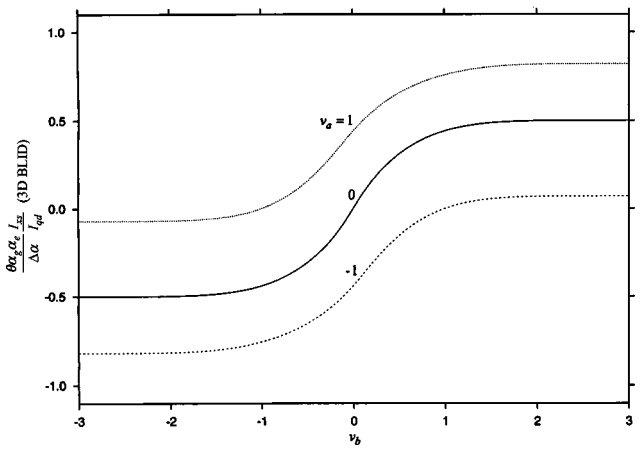

FIG. 3. As Fig. 2 except that 3D BLID is considered.

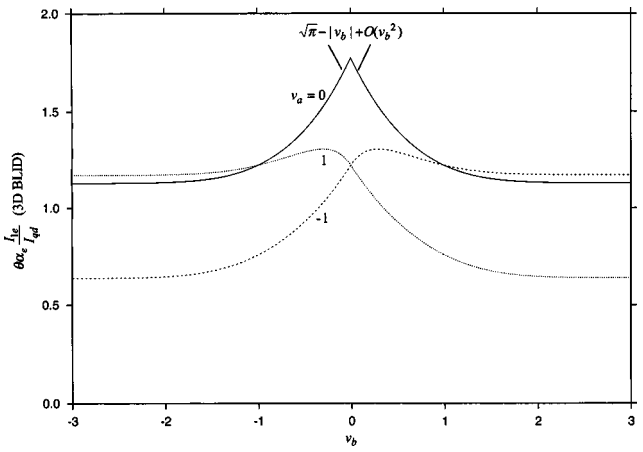

FIG. 4. As Fig. 3 except that exact results for I_{1e}/I_{qd} with $z = 1$ are shown.

Some explanation of the origins of the names used in the definitions (A10)–(A14) will help readers to remember them. The use of capital D for $D(\mathrm{erf})$ in Eq. (A10) and $D(v\ \exp)$ in Eq. (A11) alludes to the fact that the absolute values $|v_a|,|v_b|$ must be used. The notation erfc(z) is standard for the complementary error function $(1-\mathrm{erf}\,z)$, and capitalizing the "c" to "C" in Eqs. (A12) and (A13) alludes to the fact that the argument is now an absolute value; the v and v^2 are appended for the obvious reason. Similarly, $\exp \mathrm{C}(z)$ could be used for a complementary exponential function $(1-e^{-z^2})$, with the "sgn" appended in (A14), again for the obvious reason.

APPENDIX B: RESULTS FOR THE INTEGRALS FOR CASE A, THAT IS, $0 \leqslant v_a < v_b$

With the 12 definitions

$$I_{\xi 0}^{(1)} = G_{a\xi}, \tag{B1a}$$

$$I_{\xi 0}^{(2)} = dG_{\xi}, \tag{B1b}$$

$$I_{\xi 0}^{(3)} = G_{\xi} - G_{b\xi}, \tag{B1c}$$

$$I_{\xi 1}^{(1)} = \mathrm{erf}\, v_a - I_{\xi 0}^{(1)}, \tag{B2a}$$

$$I_{\xi 1}^{(2)} = d(\mathrm{erf}) - I_{\xi 0}^{(2)}, \tag{B2b}$$

$$I_{\xi 1}^{(3)} = 1 - \mathrm{erf}\, v_b - I_{\xi 0}^{(3)}, \tag{B2c}$$

$$I_{\xi 2}^{(1)} = \pi^{-1/2}(1 - e^{-v_a^2}) - \xi I_{\xi 1}^{(1)}, \tag{B3a}$$

$$I_{\xi 2}^{(2)} = \pi^{-1/2} d(\exp) - \xi I_{\xi 1}^{(2)}, \tag{B3b}$$

$$I_{\xi 2}^{(3)} = \pi^{-1/2} e^{-v_b^2} - \xi I_{\xi 1}^{(3)}, \tag{B3c}$$

$$I_{\xi 3}^{(1)} = \tfrac{1}{2}\,\mathrm{erf}\, v_a - \pi^{-1/2} v_a e^{-v_a^2} - \xi I_{\xi 2}^{(1)}, \tag{B4a}$$

$$I_{\xi 3}^{(2)} = \tfrac{1}{2} d(\mathrm{erf}) + \pi^{-1/2} D(v\ \exp) - \xi I_{\xi 2}^{(2)}, \tag{B4b}$$

$$I_{\xi 3}^{(3)} = \tfrac{1}{2}(1 - \mathrm{erf}\, v_b) + \pi^{-1/2} v_b e^{-v_b^2} - \xi I_{\xi 2}^{(3)}, \tag{B4c}$$

the results may be written as follows:

$$I_{1j} = S_j + 2W_j(I_{w2}^{(2)} - v_a I_{w1}^{(2)} + dv I_{w1}^{(3)}) + 2Z_j(2I_{g2}^{(1)} + I_{g2}^{(2)} + v_a I_{g1}^{(2)} + 2I_{g2}^{(3)} - dv I_{g1}^{(3)}), \tag{B5}$$

$$I_{qj} = [\tfrac{1}{2} S_j d(\mathrm{erf}) + 2W_j(I_{w2}^{(2)} - v_a I_{w1}^{(2)} + dv I_{w1}^{(3)})] q_0, \tag{B6}$$

$$I_{vj} = 2\pi^{-1/2} S_j + 2W_j(I_{w3}^{(2)} - v_a I_{w2}^{(2)} + dv I_{w2}^{(3)}) + 2Z_j(2I_{g3}^{(1)} + I_{g3}^{(2)} + v_a I_{g2}^{(2)} + 2I_{g3}^{(3)} - dv I_{g2}^{(3)}), \tag{B7}$$

$$I_{xj} = W_j[I_{w3}^{(2)} - v_a^2 I_{w1}^{(2)} + d(v^2) I_{w1}^{(3)}] - Z_j[I_{g3}^{(2)} - v_a^2 I_{g1}^{(2)} + d(v^2) I_{g1}^{(3)}]. \tag{B8}$$

[1] F. O. Goodman, Phys. Rev. A **65**, 063409 (2002).

[2] F. O. Goodman, Phys. Rev. A **65**, 063410 (2002).

[3] F. O. Goodman, Phys. Rev. A **67**, 013410 (2003).

[4] As in part III, we discuss the ratio I_{qd}/q_0 rather than I_{qd}/a because of the different definitions of a, in terms of the important physical quantity q_0, which have been used.

[5] For example, the exact results for the three ratios I_{qd}/q_0, I_{xs}/I_{qd}, and I_{1e}/I_{qd} have a total of more than 1700 lines using MAPLE V Release 5 (University of Waterloo, Waterloo Maple Inc.), although this could no doubt be reduced with some effort.

[6] M. A. Vaksman and I. Podgorski, Can. J. Phys. **74**, 25 (1996).